

Search for exoplanets in M31 with pixel-lensing and the PA-99-N2 event revisited

Gabriele Ingresso · Sebastiano Calchi Novati ·
Francesco De Paolis · Philippe Jetzer ·
Achille Nucita · Alexander Zakharov

Received: date / Accepted: date

Abstract Several exoplanets have been detected towards the Galactic bulge with the microlensing technique. We show that exoplanets in M31 may also be detected with the pixel-lensing method, if telescopes making high cadence observations of an ongoing microlensing event are used. Using a Monte Carlo approach we find that the mean mass for detectable planetary systems is about $2 M_J$. However, even small mass exoplanets ($M_P < 20 M_\oplus$) can cause significant deviations, which are observable with large telescopes. We reanalysed the POINT-AGAPE microlensing event PA-99-N2. First, we test the robustness of the binary lens conclusion for this light curve. Second, we show that for such long duration and bright microlensing events, the efficiency for finding planetary-like deviations is strongly enhanced with respect to that evaluated for all planetary detectable events.

Keywords Microlensing · Exoplanets · Spiral galaxies: M31

PACS 95.75.De · 97.82.-j · 98.62.Sb

Gabriele Ingresso

Dipartimento di Fisica, Università del Salento, and *INFN* Sezione di Lecce, I-73100 Lecce, Italy, E-mail: ingrosso@le.infn.it

Sebastiano Calchi Novati

Dipartimento di Fisica, Università di Salerno, and *INFN* Sezione di Napoli, I-84081 Baronissi, Italy, E-mail: novati@sa.infn.it

Francesco De Paolis

Dipartimento di Fisica, Università del Salento and *INFN* Sezione di Lecce, CP 193, I-73100 Lecce, Italy, E-mail: depaolis@le.infn.it

Philippe Jetzer

Institute for Theoretical Physics, University of Zürich, Winterthurerstrasse 190, CH-8057 Zürich, Switzerland, E-mail: jetzer@iftp.uzh.ch

Achille Nucita

XMM-Newton Science Operations Centre, ESAC, ESA, PO Box 50727, 28080 Madrid, Spain, E-mail: achille.nucita@sciops.esa.int

Alexander Zakharov

Institute of Theoretical and Experimental Physics, B. Chermushkinskaya 25, 117259 Moscow, and Bogoliubov Laboratory of Theoretical Physics, Joint Institute for Nuclear Research, 141980 Dubna, Russia, E-mail: zakharov@itep.ru

1 Introduction

Gravitational microlensing technique initially developed to search for MACHOs in the Galactic halo can be used to infer the presence of exoplanets around lens stars [1,2]. Indeed, the planet orbiting the primary lens star may induce significant perturbations to the standard (single lens) Paczyński like microlensing light curves [3,4]. Until now, 10 exoplanets has been detected towards the Galactic bulge (see <http://exoplanet.eu>) and the least massive planets have masses of about 3, 5 and 13 M_{\oplus} . The planet orbital separations are in the range 2–5 AU (about the Einstein ring radius). Microlensing technique complements the planet detections by other methods (Doppler radial velocity measurements and transits are among the most efficient) ¹ that are more sensitive to large planet masses (Jupiter-like planets) at small orbital distances. Microlensing gives also the opportunity to detect planets lying in M31 [5,6]. In this case, however, the source stars are not resolved by ground based telescopes, a situation referred to as “pixel-lensing” [7,8,9,10]. Until now, however, only 25 microlensing events have been observed towards M31 [11] and in one case a deviation of the microlensing light curve from the standard Paczyński shape has been observed and attributed to a secondary component orbiting the lens star [12]. However, new observational campaigns towards M31 have been undertaken [13,14,15] and hopefully new exoplanets might be detected in the future.

The possibility to detect planets in pixel-lensing observations towards M31 has been already explored [5,16,17]. The analysis for planet detection, however, has been performed by using a fixed configuration of the underlying Paczyński light curve. In the present work, using a Monte Carlo (MC) approach [18] we explore chances to detect exoplanets in M31, by considering the multi-dimensional space of parameters for both lensing and planetary systems. By using the method of residuals, we select the light curves that show detectable deviations with respect to the Paczyński shape. The advantage of the MC approach is that of allowing a detailed characterisation of the sample of microlensing events for which the planetary deviations are more likely to be detected.

2 Generation of Planetary Microlensing Events

Assuming that the lens is a planetary system lying in the M31 bulge or disk we generate a sample of pixel-lensing events towards M31. Microlensing parameters are selected according to the method outlined in [19,20,21]. To select planetary parameters (mass M_P and orbital period P) we adopt the relation [22]

$$dn(M_P, P) \propto M_P^{-\alpha} P^{-\beta} \left(\frac{dM_P}{M_P} \right) \left(\frac{dP}{P} \right) , \quad (1)$$

with $\alpha = 0.11$ and $\beta = -0.27$. This relation was obtained by investigating the distribution of masses and orbital periods of 72 exoplanets (detected mainly by Doppler radial velocity method), and taking into account the selection effects caused by the limited velocity precision and duration of existing surveys ². The upper limit of the

¹ At the moment about 400 exoplanets have been discovered, basically at relatively small distances from the Earth (see <http://exoplanet.eu>).

² A recent re-analysis [23] of the mass-period relation employing a larger catalog of 175 exoplanets detected by the Doppler radial velocity method is consistent with that of [22].

planetary mass is set at $10 M_J$ which roughly corresponds to the lower mass limit for brown dwarfs. Moreover, following the numerical simulations for the planetary system formation [24], we set the lower planetary mass limit at $M_P = 0.1 M_\oplus$. Once the masses of the binary components and the planet period have been selected, the binary separation d_P is obtained by assuming a circular orbit. We also suppose that planetary perturbation time scales are much shorter than orbital periods of planets. All distances are normalised to the Einstein radius R_E of the total mass M of the lens system

$$R_E = \sqrt{\frac{4GM}{c^2} \frac{D_S - D_L}{D_S}}, \quad (2)$$

where D_S (D_L) is the source (lens) distance. Moreover, it is assumed that all stars in M31 have planets.

We simulate pixel-lensing light curves assuming a regular sampling (between 2 and 24 hours), telescopes of different diameters in the range 2 – 8 m, typical observational conditions and an exposure time t_{exp} of 30 and 60 min. Moreover, since in pixel-lensing towards M31 the bulk of the source stars are red giants (with large radii), we take into account the source finiteness by averaging the planetary magnification $A_P(t_i)$ (numerically evaluated by using the binary lens equation [25,26]) on the source size. A microlensing light curve is given by

$$S_P(t_i) = f_{\text{bl}} + f_0[\langle A_P(t_i) \rangle - 1], \quad (3)$$

where f_{bl} is the background signal from M31 and the sky, f_0 is the unamplified source star flux and $\langle A_P(t_i) \rangle$ the time varying magnification, that is averaged on the (projected) source size Σ

$$\langle A_P(t_i) \rangle = \frac{\int_0^{2\pi} d\theta \int_0^\rho A_P(\tilde{\theta}, \tilde{\rho}; t_i) I(\tilde{\rho}) \tilde{\rho} d\tilde{\rho}}{2\pi \int_0^\rho I(\tilde{\rho}) \tilde{\rho} d\tilde{\rho}}, \quad (4)$$

where $\rho = \theta_S/\theta_E$ is the normalised angular size of the source ($\theta_S = R_S/D_S$, R_S being the source radius, $\theta_E = R_E/D_L$ is the angular Einstein radius) and $I(\tilde{\rho})$ the intensity profile of the source including limb darkening (see [18] for more details).

Planetary perturbations in the light curves occur when the source star trajectory in the lens-plane (the plane orthogonal to the line of sight to the M31 star source, passing at the lens position) crosses and/or passes near caustics. This is the caustic set of the source positions at which the magnification is infinite in the ideal case of a point source. Clearly for realistic sources of finite size the magnification gets still large, but finite.

Light curves that show significant ($> 3\sigma$) flux variations with respect to the background noise in at least three points identify a sample of “detectable” events. These curves are fitted with a standard Paczyński form

$$S^0(t) = f_{\text{bl}}^0 + f_0^0[\langle A^0(t_i) \rangle - 1], \quad (5)$$

where $\langle A^0(t_i) \rangle$ is the usual magnification for a single lens and the averaging is made on the projected source size ρ .

Next, to select light curves with detectable planetary features we consider two indicators: (i) the overall deviation (in units of error-bars) of the planetary light curves from the corresponding Paczyński best fit, as measured by the sum of residuals $\chi_r^2 = \sum_i \chi_r^2(t_i)/N_{\text{tot}}$ (N_{tot} is the total number of points) and (ii) the number of points

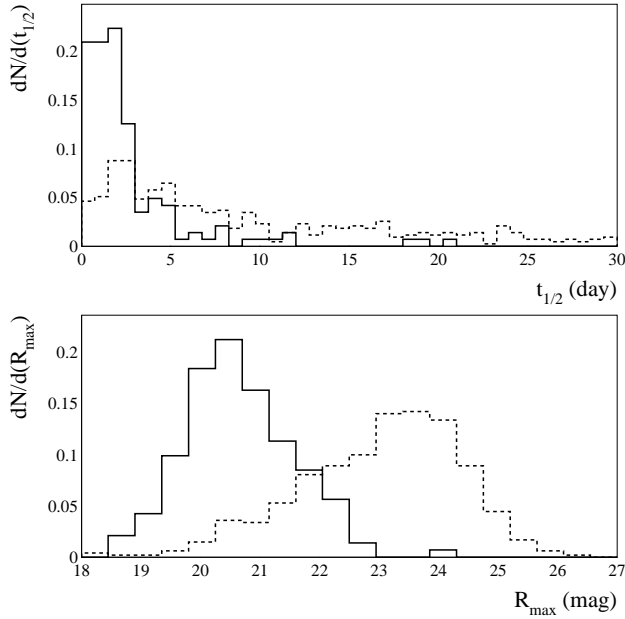


Fig. 1 Normalised (to unity) distributions of $t_{1/2}$ (top panel) and R_{\max} (bottom panel) for planetary selected events with $\chi_r > 4$, $N_{\text{good}} > 3$ and $\langle \epsilon \rangle_{\max} > 0.1$. Here and in the following figures we select the following parameters: telescope diameter $D=8$ m, an exposure time $t_{\text{exp}} = 30$ min, a sampling time of the light curve of 2 hours. Solid lines correspond to I class events, dashed lines to II class events.

N_{good} , even not consecutive, which deviate significantly from the Paczyński fit. By a direct survey of many light curves we fix the thresholds $\chi_r \text{ th} = 4$ and $N_{\text{good th}} = 3$ and we select a sub-sample of light curves with detectable planetary features having $\chi_r^2 > 4$ and $N_{\text{good}} > 3$. However, in this way, we find that some of the selected light curves show overall distortions (with respect to the Paczyński shape) which hardly could be attributed in real observations to a planet orbiting the primary lens star (we mean that it is not easy to reconstruct parameters of planetary systems from such observational data). This happens, in particular, for events with small planetary mass and/or large (projected) source radius, for which the finite source effects are maximised. A measure of the relevance of these effects is given by the relative (with respect to the Paczyński value) planetary magnification averaged on the source area

$$\langle \epsilon(t_i) \rangle = \left(\frac{\int_{\Sigma} d^2 \mathbf{x} [|A_P(\mathbf{x}, t_i) - A^0(\mathbf{x}, t_i)| / A^0(\mathbf{x}, t_i)]}{\int_{\Sigma} d^2 \mathbf{x}} \right). \quad (6)$$

To be conservative, events with maximal finite source effects are eliminated from the following analysis by requiring, besides conditions (i) and (ii), that (iii) $\langle \epsilon \rangle_{\max} > 0.1$, where $\langle \epsilon \rangle_{\max}$ is the maximum value of $\langle \epsilon(t_i) \rangle$ along the whole light curve. Conditions (i) and (ii) are particularly efficient to select light curves with a large number of points

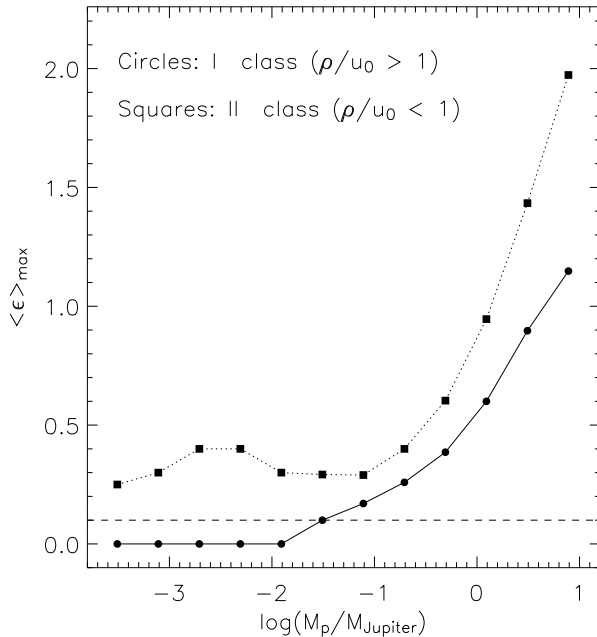


Fig. 2 The maximum relative planetary magnification $\langle \epsilon \rangle_{\max}$ is given as a function of M_P .

deviating from the Paczyński best fit, the condition (iii) ensures the presence on the light curve of at least one clear planetary feature.

3 Results

In Fig. 1 (for $D = 8$ m), we give the distributions of $t_{1/2}$ and R_{\max} for the events with detectable planetary deviations ($\chi_r^2 > 4$, $N_{\text{good}} > 3$ and $\langle \epsilon \rangle_{\max} > 0.1$). Here, $t_{1/2}$ is the full-width half-maximum microlensing event duration $t_{1/2} = t_E f(u_0)$, where $f(u_0)$ is a function [9] of the dimensionless impact parameter u_0 and R_{\max} is the magnitude in the R -band corresponding to the flux variation at the maximal Paczyński **magnification** $\Delta f_{\max}^0 = f_0^0(A_{\max}^0 - 1)$. In the Fig. 1 we discriminate two classes of events (indicated by I and II), according to the ratio $\rho/u_0 > 1$ (solid lines) or $\rho/u_0 < 1$ (dashed lines). The events of the I class with $\rho/u_0 > 1$ have short time durations ($\langle t_{1/2} \rangle \simeq 1.6$ day) and larger flux variations ($\langle R_{\max} \rangle \simeq 20.6$ mag). In these events planetary deviations are caused by the source trajectory crossing (in the lens plane) the central caustic region, close to the primary lens star. The events of the II class, with $\rho/u_0 < 1$, have longer durations ($\langle t_{1/2} \rangle = 6.4$ day) and smaller flux variations ($\langle R_{\max} \rangle = 23.1$ mag). Planetary perturbations in these cases are (mainly) caused by the intersection of the source trajectory with the planetary caustics and may also appear at times far from the maximum magnification time t_0 .

The fraction of I class events is about 5%. However, it turns out that the probability to have detectable planetary features in these events (that however are rare)

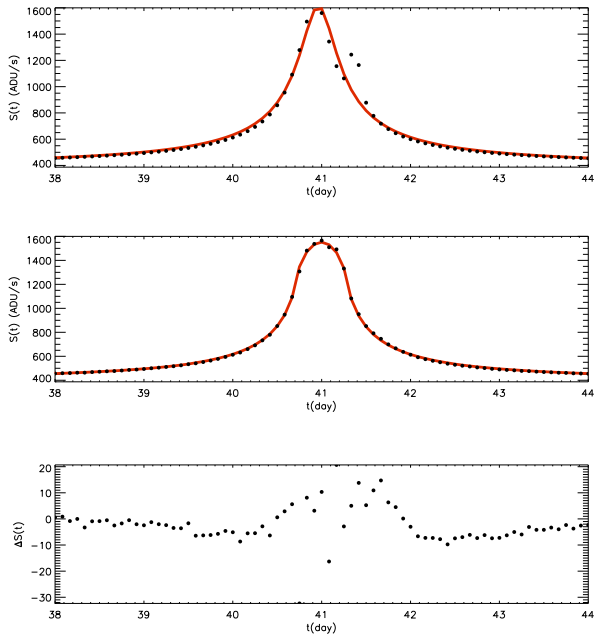


Fig. 3 Simulated I class event (points) and Paczyński fit (solid line). Some parameter values: $\rho/u_0 = 2.14$, $R_{\max} = 19.0$ mag, $t_{1/2} = 0.6$ day, $M_P = 1.04 M_J$, $M = 0.55 M_\odot$ (M is the total mass of the lens system), $d_P = 3.6$ AU, $R_E = 5.55$ AU, $\chi_r = 46$, $\langle \epsilon \rangle_{\max} = 0.2$.

is higher. This happens since the crossing of the central caustic is more probable in I class events with $\rho/u_0 \gg 1$. On the contrary, the generated events of the II class are more numerous, but have a smaller probability to show detectable planetary features.

The existence of the two classes of planetary events in pixel-lensing towards M31 is also evident in the Fig. 2, where we show $\langle \epsilon \rangle_{\max}$ (averaged on a large number of MC events of the same planetary mass M_P) as a function of M_P . We find that $\langle \epsilon \rangle_{\max}$ increases with increasing M_P , a result that is expected since the size of the caustic region is increasing with the planetary mass [28, 29, 30]. We also verify that the finite size effects are more important for I class events. Indeed, for a given mass M_P , the events of the I class (with $\rho/u_0 > 1$) have smaller values of $\langle \epsilon \rangle_{\max}$ with respect to the corresponding II class events.

An example of light curve for a I class event is shown in the central panel of the Fig. 3. Here, we can see how the planetary deviations in the light curve (upper panel) obtained by using the point-like source approximation are washed out when the magnification is averaged on the source area (second panel). However, also in this case, planetary deviations, as measured by the residuals (bottom panel), still are present. The planetary event MOA-2007-BLG-400 shows a similar shape of the light curve [31].

An example of II class event is given in Fig. 4 where we see that also a small mass planet ($M_P = 0.3 M_\oplus$) can cause detectable planetary deviations in events for which the finite size effects are small (see also Fig. 8 in paper [4]; we remind that we have local light minima in the cases $d_P < R_E$). In the considered event the geometry is such

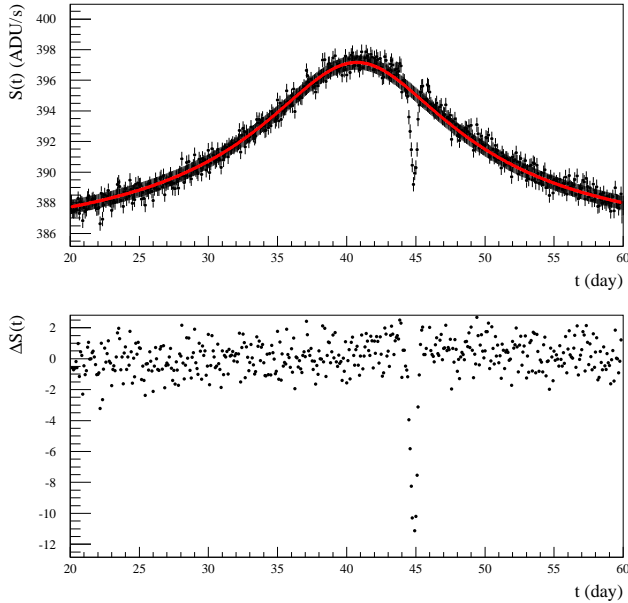


Fig. 4 Simulated II class event (points) and Paczyński fit (thin solid line). Some parameter values: $\rho/u_0 = 0.04$, $R_{\max} = 24.0$ mag, $t_{1/2} = 18.7$ day, $M_P = 0.3 M_{\oplus}$, $M = 0.31 M_{\odot}$ (M is the total mass of the lens system), $d_P = 3.8$ AU, $R_E = 3.3$ AU, $\chi_r = 8.0$, $\langle \epsilon \rangle_{\max} = 0.4$.

that the source trajectory is passing (in the lens plane) in the region between the two planetary caustics, where a deficit of magnification is present. Other examples of light curves for I and II class events are given in [18].

The distributions of the planet mass M_P for the planetary selected events ($\chi_r^2 > 4$, $N_{\text{good}} > 3$ and $\langle \epsilon \rangle_{\max} > 0.1$) is given in the Fig. 5 (solid line). For comparison, the M_P distribution for the whole sample of detectable events (dashed line) is also given. From Fig. 5 it follows that larger planetary masses lead to higher probability for the detection of planetary features. This result reflects the fact that the detection probability is proportional to the caustic area (for small size sources), which increases with the planet-to-star mass ratio. From the same figure, it also follows that the exoplanet detection can occur with a non negligible probability for $M_P > 0.06 M_J$ ($M_P > 20 M_{\oplus}$), although even Earth mass exoplanets might be in principle detectable. However, if we consider telescopes with smaller diameter ($D < 4$ m), the tail at low masses in Fig. 5 disappears and, practically no exoplanet detection occurs for $M_P < 0.06 M_J$.

The probability of planet detection is maximised when the planet-to-star separation d_P is inside the so called “lensing zone”, which is the range of star-to-planet separation $0.6 < d_P/R_E < 1.6$ [27,28]. The d_P distribution for selected (solid line) and detectable (dashed line) events are shown in the upper panel of Fig. 6. The relevance of the lensing zone is clarified in the bottom panel of the same figure where the planet separation (in unit of the Einstein radius) $d = d_P/R_E$ is plotted.

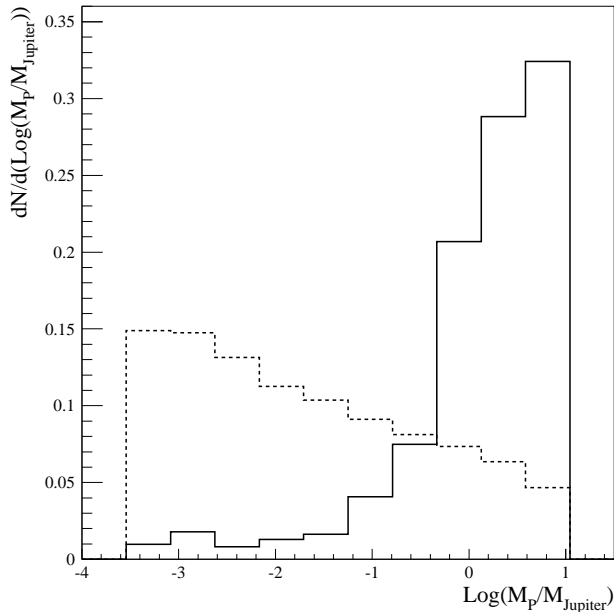


Fig. 5 Normalised (to unity) distributions of the exoplanet mass M_P for the events with detectable planetary deviations (solid line) and for the generated events (dashed line).

Our analysis shows that in pixel-lensing searches towards M31 the typical duration of planetary perturbations is about 1.4 days. However, the number of significant planetary deviations on each light curve increases with increasing ratios ρ/u_0 . So, the overall time scale for planetary deviations can increase up to 3 – 4 days (for I class events). This means that a reasonable value of the time step for pixel-lensing observations aiming to detect planets in M31 is a few (4–6) hours, almost irrespectively on the telescope diameter D .

We also verify that the overall probability (we stress that here we are considering the full planetary mass range from $0.1 M_\oplus$ until $10 M_J$, as well as the R_{\max} and $t_{1/2}$ ranges) to find pixel-lensing events with detectable planetary deviations is, however, very small: less than 2 % for $D = 8$ m and about 3%, if in the selection procedure we relax condition (iii) (namely, $\langle \epsilon \rangle_{\max} > 0.1$) and decreases rapidly for smaller telescopes.

4 Analysis of the PA-99-N2 event case

The POINT-AGAPE collaboration reported the detection of the microlensing event PA-99-N2 [32]. This appears as a peculiar event first because of its extreme brightness ($R_{\max} \simeq 19$ mag), long duration ($t_{1/2} \simeq 24$ day)³ and location, some 22 arcmin away from the M31 center; second, as shown in a subsequent analysis [12], because the

³ As discussed in Section 3, for the II class events the mean values of R_{\max} and $t_{1/2}$ are about 23.1 mag and 6.4 day, respectively.

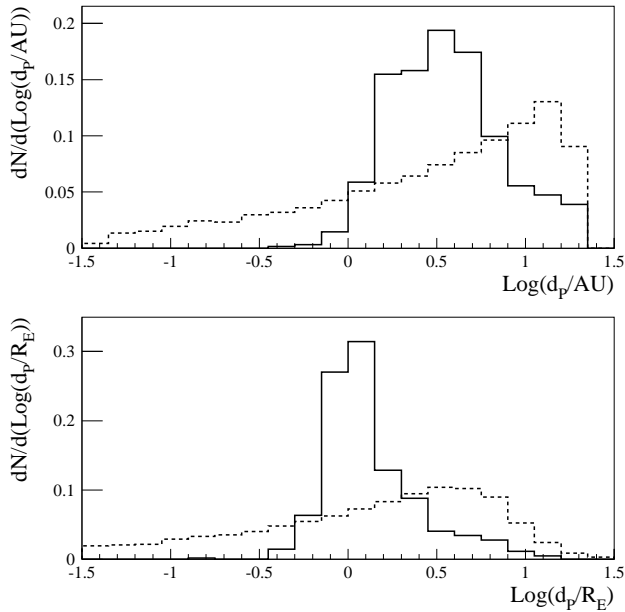


Fig. 6 Upper panel: normalised (to unity) distributions of the star-to-planet separation d_p (in AU units) for the events with detectable planetary deviations (solid line) and for the generated events (dashed line). Bottom panel: distribution of d_p/R_E for events as before.

anomaly with respect to the Paczyński shape along the light curve can be attributed to a secondary component orbiting the lens star. In particular, An et al. [12] have evaluated the *a posteriori* probability distribution for the lens mass which results to be extremely broad: for source and lens disc objects, they report a lens mass range $0.02 - 3.6 M_\odot$ at 95% confidence level. Together with the small best fit binary lens mass ratio, $q \simeq 1.2 \times 10^{-2}$, this puts the lens companion well in the substellar range. In paper [18] we have remarked that taking at face value the most likely value for the lens mass $\simeq 0.5 M_\odot$ for a disc lens, the lens companion would be a $\simeq 6.34 M_J$ object. This would make of the PA-99-N2 lens companion the first exoplanet discovered in M31. Furthermore, we had analysed the PA-99-N2 event within the framework of our simulation scheme, showing in particular that its (microlensing and planetary) parameters nicely fall in the expected range for II class events [18]. Here we further analyse this event. First, starting from the observational data⁴, we test the robustness of the binary-lens best fit solution. Second, we address the question of the efficiency for finding binary-like deviations for such bright and long duration events.

In Table 1 of An et al. [12] a list of the best fit parameters adopting various models, including the best fit assuming a single lens, for different location of the lens system are given. In particular, the two best fit binary models, named C1 and W1,

⁴ Courtesy of the POINT-AGAPE collaboration.

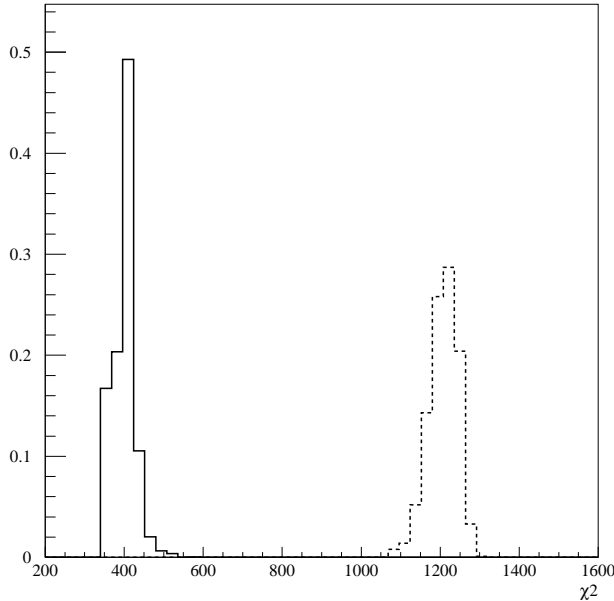


Fig. 7 Normalised (to unity) distributions of the χ^2 for binary (solid line) and single lens fit (dashed line).

are indistinguishable⁵ in terms of their χ^2 . An et al. [12] considered finite source corrections for the C1 model (they named this model as FS) and found that these corrections decrease slightly the χ^2 ($\simeq 2\%$) with respect to C1 model. Therefore, these authors claimed that C1 and FS models are practically the same. In our analysis we consider the C1 model. To verify the robustness of the binary-lens fit solution, the first test is to add a Gaussian noise to the best fit of the observed light curve to verify if a single lens model with noise can reproduce the observational data. We also let each parameter vary (by at most 20%) around the given central value. For each of the so obtained light curve we calculate the χ^2 , which is plotted in Fig. 7 (dashed line). We have verified that the lowest χ^2 value corresponds to the parameters of the best fit Paczyński model (last row) in Table 1 of An et al. [12]. Similarly, we have taken the best fit binary model C1 and realised more than one thousand models by adding Gaussian noise and letting the parameters to vary by at most 20%. We plot again in Fig. 7 the χ^2 distribution (solid line). Also here the lowest χ^2 value is obtained for the C1 model without noise. Moreover, from Fig. 7 one can see that the two (normalized) distributions of the χ^2 are clearly separated, which implies that the best single lens fit is much worse than any of the binary lens models. From this we conclude that the binary fit is robust and that the observed light curve cannot be obtained by any single lens model with random noise.

⁵ There exist several binary lens models that lie at a local χ^2 minimum. Some of these degeneracy would have been removed if the $\simeq 20$ day observation gap between JD' 72 and JD' 91 had been regularly covered [12].

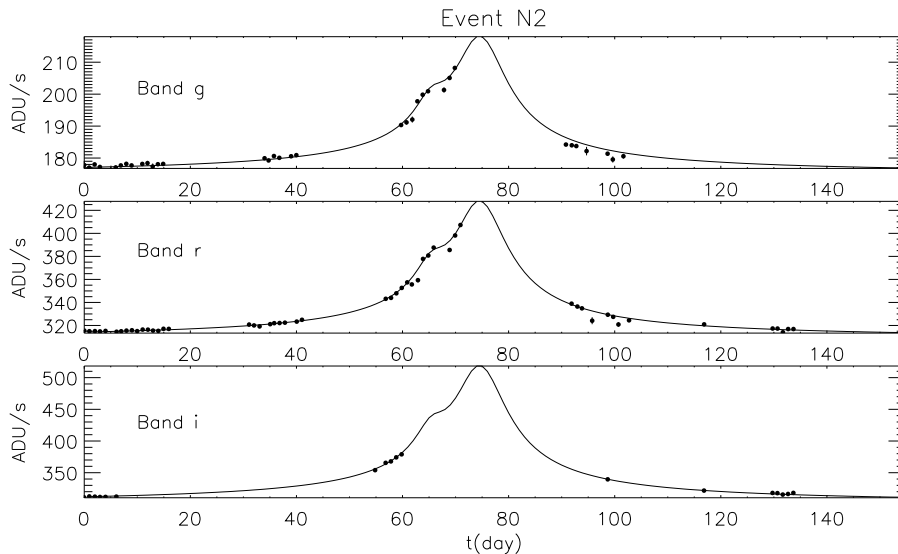


Fig. 8 The binary light curves corresponding to the C1 model [12] for g, r and i bands.

A further point to be stressed is the following: at the end of the previous section we have mentioned that the probability to detect an exoplanet in pixel-lensing observations towards M31 is rather small even with large telescopes. Therefore, the question which arises now is the following: what is the chance of finding a planetary feature in an event as PA-99-N2? The basic answer can be found looking at the characteristics of the underlying microlensing event. As it is also apparent by comparing with the distributions shown in Fig. 1, this is, at the same time, an extremely bright and long duration event. In fact, as we now show, this strongly enhances the probability for finding deviations to the single lens shape. To this purpose we perform a MC simulation where we fix the single lens parameters R_{\max} and $t_{1/2}$ to those of PA-99-N2 and we let vary the binary ones (planet-to-star mass ratio, planetary distance in unit of R_E and orientation of the source trajectory with respect to the binary axis) for an observational setup fixed to reproduce that of the POINT-AGAPE observations (mirror size, sampling and exposure time). In particular we find, for the selected planetary mass range, an increase of the average efficiency up to 6%, to be compared with less than 0.6% (see Table 3 in [18]) for events without any constraints on R_{\max} and $t_{1/2}$. Moreover, as also implicit from the analysis of Fig. 5, the efficiency for finding binary-like deviations in the simulated light curves increases significantly with the lens-companion mass. In particular, for the restricted range $1 - 10M_J$ we find the average efficiency rises up to 27%. We have restricted our attention to the planetary-mass range for the lens companion ($M_P < 10 M_J$ was our initial assumption), but we might expect the efficiency still rises once we enter the brown dwarf mass range (as in fact it is allowed by the analysis [12]). Finally, the efficiency would be further enhanced for a lens-companion mass function more peaked towards higher values of the mass than that we have assumed.

5 Conclusions

We have discussed the possibility to detect planets in M31 by using pixel-lensing observations with telescopes of different sizes and observational strategies. Assuming that each lens star is hosting a planet, we carry out MC simulations and explore the multi-dimensional space of the parameters for both the lensing and planetary systems. Planetary induced perturbations in light curves are detected by comparing the simulated light curves with the corresponding Paczyński shapes and searching for significant deviations. The MC approach allows to characterise the sample of events for which the planet detections are more likely to be observed. Since in pixel-lensing towards M31 the bulk of the source stars are red giant (with large radii), we take into account the finite source effects, which induce a smoothing of the planetary deviations and decrease thus the chance to detect planets. We estimate the typical duration of a single planetary feature to be of about one day. However, the number of significant planetary deviations and consequently the overall time scale of the perturbations increases (up to a few days), increasing the source size. Therefore for pixel-lensing searches towards M31 only few exposures per day could be enough to detect planetary features in light curves. Pixel-lensing technique favours the detection of large mass planets ($M_P \simeq 2 M_J$), even if planets with mass less than $20 M_\oplus$ could be detected, although with small probability, by using large telescopes with a sufficient photometric stability.

As a test case for exoplanetary searches in M31 we have reconsidered the POINT-AGAPE event PA-99-N2, which had already been probed to show an anomaly with respect to the Paczyński shape compatible with a binary lens. As a first step we have revisited the issue of the single lens versus binary lens solution, finding that the latter is indeed robust against the introduction of a gaussian noise along the observed data. According to the previous POINT-AGAPE analysis this binary system has a small mass ratio and this makes at least plausible that the lens companion is indeed an exoplanet. Furthermore, the underlying microlensing event is extremely, and somewhat unusually, long and bright. Therefore, as a second step, we have carried out a specific MC simulation that allowed us to show that for this kind of events the chance of finding exoplanetary deviations is indeed greatly enhanced and possible even for an observational set up as that of the POINT-AGAPE observations. As a caveat, we mention that the efficiency grows with the lens companion mass also beyond the exoplanet mass range in the brown dwarf one.

Whatever the case for PA-99-N2 event, our analysis confirms that looking for exoplanets in M31 with pixel-lensing, at least in the Jupiter mass range, is already reachable with present technology. Clearly, an efficient strategy of search, as towards the Galactic bulge, is mandatory: a wide field survey, to collect a large enough number of pixel-lensing candidates, endowed with an early warning system to trigger subsequent follow up observations, possibly with a network of telescopes around the world (for which also telescopes with small field of view could be usefully employed). In our opinion the reward of such a project would be substantial: going from the settling of the question of the MACHO fraction in M31 halo, to important information on the stellar mass function and the detection of exoplanets, besides other information on the M31 structure and content of variable stars.

Acknowledgements SCN acknowledges support for this work by the Italian Space Agency (ASI) and by the “Istituto Internazionale per gli Alti Studi Scientifici” (IIASS). AFZ thanks a financial support by INFN (Sezione di Lecce) at Dipartimento di Fisica (Salento University).

References

1. Gould, A.: Recent Developments in Gravitational Microlensing, In K. Stanek, K., (ed.) *The Variable Universe: A Celebration of Bohdan Paczyński*, ASP Conference Series, USA. San Francisco: Astronomical Society of the Pacific, 2009, p. 86; arXiv:0803.4324v1 [astro-ph]
2. Bennett, D.: Detection of Extrasolar Planets by Gravitational Microlensing, arXiv:0902.1761v1 [astro-ph.EP]
3. Mao, S., & Paczyński, B.: Gravitational microlensing by double stars and planetary systems, *ApJ*, 374, L37 (1991)
4. Paczyński, B.: Gravitational Microlensing in the Local Group, *ARA&A* (1996)
5. Covone, G., de Ritis, R., Dominik, M. & Marino, A. A.: Detecting planets around stars in nearby galaxies, *A&A* 357, 816 (2000)
6. Baltz, E. A. & Gondolo, P.: Binary Events and Extragalactic Planets in Pixel Microlensing, *ApJ*, 559, 41 (2001)
7. Crots, A. P. S.: M31 - A unique laboratory for gravitational microlensing, *ApJ*, 399, L43 (1992)
8. Baillon, P., Bouquet, A., Giraud-Heraud, Y. & Kaplan J.: Detection of Brown Dwarfs by the Microlensing of Unresolved Stars, *A&A*, 277, 1 (1993)
9. Gould, A.: Theory of Pixel Lensing, *ApJ*, 470, 201 (1996)
10. Ansari, R., et al.: AGAPE: a search for dark matter towards M31 by microlensing effects on unresolved stars?, *A&A*, 324, 843 (1997)
11. Calchi Novati, S.: Pixel-lensing: microlensing towards M31, arXiv:0912.2667 (2009)
12. An J.H., et al.: The Anomaly in the Candidate Microlensing Event PA-99-N2, *ApJ*, 601, 845 (2004)
13. Kerins, E. et al: The Angstrom Project: a microlensing survey of the structure and composition of the bulge of the Andromeda galaxy, *MNRAS*, 365, 1099 (2006)
14. Riffesser A., Seitz S., Bender, R.: The M31 Microlensing Event WeCAPP-GL1/POINT-AGAPE-S3: Evidence for a MACHO Component in the Dark Halo of M31? *ApJ*, 684, 1093 (2008)
15. Calchi Novati S., et al.: Candidate Microlensing Events from M31 Observations with the Loiano Telescope, *ApJ*, 695, 442 (2009)
16. Chung, S.-J., et al.: The Possibility of Detecting Planets in the Andromeda Galaxy, *ApJ*, 650, 432 (2006)
17. Kim, D., et al.: Detection of M31 Binaries via High-Cadence Pixel-lensing Surveys, *ApJ*, 666, 236 (2007)
18. Ingresso, G. et al.: Pixel-lensing as a way to detect extrasolar planets in M31, *MNRAS*, 399, 219 (2009)
19. Kerins, E., et al.: Theory of pixel lensing towards M31 - I. The density contribution and mass of MACHOs, *MNRAS*, 323, 13 (2001)
20. Ingresso, G. et al.: Monte Carlo analysis of MEGA microlensing events towards M31, *A&A*, 445, 375 (2006)
21. Ingresso, G. et al.: A new analysis of the MEGA M 31 microlensing events, *A&A*, 462, 895 (2007)
22. Tabachnik S., & Tremaine S.: Maximum-likelihood method for estimating the mass and period distributions of extrasolar planets, *MNRAS*, 335, 151 (2002)
23. Jiang, I.-G. et al.: On the fundamental mass-period functions of extrasolar planets, arXiv:0912.2585v1 (2009)
24. Ida, S. and Lin D.N.C.: Toward a Deterministic Model of Planetary Formation. II. The Formation and Retention of Gas Giant Planets around Stars with a Range of Metallicities, *ApJ*, 616, 567 (2004)
25. Witt, H. J.: Investigation of high amplification events in light curves of gravitationally lensed quasars, *A&A*, 236, 311 (1990)
26. Witt, H. J., & Mao, S.: On the Minimum Magnification Between Caustic Crossings for Microlensing by Binary and Multiple Stars, *ApJ*, 447, L105 (1995)
27. Griest, K. & Safizadeh N.: The Use of High-Magnification Microlensing Events in Discovering Extrasolar Planets, *ApJ*, 500, 37 (1998)
28. Gould A. & Loeb A.: Discovering planetary systems through gravitational microlenses, *ApJ*, 396, 104 (1992)
29. Zakharov A.F. & Sazhin, M.V.: Gravitational microlensing, *Physics – Uspekhi* 41, 945, (1998)
30. Bozza V.: Perturbative analysis in planetary gravitational lensing, *A&A*, 348, 311 (1999)

31. Dong S. et al.: Microlensing Event MOA-2007-BLG-400: Exhuming the Buried Signature of a Cool, Jovian-Mass Planet, *ApJ* 698, 1826 (2009)
32. Paulin-Henriksson, S. et al.: The POINT-AGAPE survey: 4 high signal-to-noise microlensing candidates detected towards M 31, *A&A* 405, 15 (2003)